NAL PROPOSAL No. 155

Scientific Spokesman:
M. L. Stevenson
Experimental Physics
Lawrence Radiation Lab
Berkeley, Calif. 94720

# Proposal to Develop a Phase I External Muon Identifier (EMI) for Use with the NAL 30 $m^3$ Bubble Chamber

R. J. Cence, F. A. Harris, M. W. Peters,
V. Z. Peterson, V. J. Stenger, and D. E. Yount
University of Hawaii

S. I. Parker, F. T. Solmitz, and M. L. Stevenson
Lawrence Radiation Laboratory

July 15, 1971

NAL PROPOSAL NUMBER 9C

# PROPOSAL TO DEVELOP A PHASE I EXTERNAL MUON IDENTIFIER (EMI) FOR USE WITH THE NAL 30 $m^3$ BUBBLE CHAMBER

R. J. Cence, F. A. Harris, M. W. Peters,
V. Z. Peterson, V. J. Stenger, and D. E. Yount
University of Hawaii

and

S. I. Parker, F. T. Solmitz, and M. L. Stevenson
University of California
Lawrence Radiation Laboratory

July 15, 1971

CONTENTS


| | | Page |
|---|---|---|
| I. | INTRODUCTION | 1 |
| II. | PHYSICS JUSTIFICATION | 3 |
| III. | PHASE I EXTERNAL MUON IDENTIFIER | 6 |
| IV. | FEASIBILITY STUDIES | 10 |
| | A. Shower-Range Data from the SLAC 20-GeV Spectrometer | 10 |
| | B. Tests for an EMI Using Proportional Chambers | 13 |
| V. | SCHEDULES AND FUNDING | 19 |

## ABSTRACT

We propose to build a Phase I External Muon Identifier for use with the NAL 30 $m^3$ bubble chamber. The Phase I EMI consists of: 1) a passive internal absorber filling the space between the magnet coils and matching the coil thickness in collision lengths (3.2 collision lengths stainless steel subtending up to 180° horizontally and weighing 20 tons), and 2) a single active external detector plane using proportional chambers to provide x, y, and diagonal information. Test data summarized in this proposal indicate that at 4 GeV/c the Phase I EMI will reject incident pions with (94±1)% efficiency while accepting 96% of the incident muons. Further, these efficiencies vary slowly with particle momentum. The construction cost to NAL of this development is estimated as $120K.

# I. INTRODUCTION

The importance of muon identification in experiments involving neutrino interactions in a bubble chamber has been emphasized in several National Accelerator Laboratory summer studies.[1] In particular, only a very small fraction of the $\nu$ interactions can be analyzed in detail without an EMI. A number of NAL proposals[2] also discuss this possibility, and two proposals explicitly describe methods for achieving this goal, one internally[3] and the other externally.[4] More recently, participants at the March 12-13, 1971, NAL 15-foot Bubble Chamber Workshop[5] were in "general agreement on the need for a muon identifier covering a large solid angle with good efficiency." These participants concluded that an identifier external to the bubble chamber would serve as a general purpose device for all known users, providing that a pion rejection of around 99% could be achieved.

Early estimates[1,4] of the absorber thickness required to distinguish muons from hadrons assumed a classic range detector, such as that used in the SLAC 20-GeV spectrometer, and arrived at values in the neighborhood of 15 collision lengths, equivalent to nearly 2 m of iron. A thick absorber is required in the simple range detector largely because the occurrence of an hadronic interaction is not apparent until all of the charged secondaries have been absorbed. This limitation can be overcome by using detectors with sufficient spatial

resolution to distinguish the large-angle scatters and multi-prong topologies associated with hadronic interactions. The bubble chamber itself is an excellent example of such a high-resolution detector, and the internal muon identifier of NAL Proposal #53[3] requires a thickness of only 1 m lead, equivalent to 1.08 m iron.

For the Phase I External Muon Identifier, we propose to use the magnet coils, plus a matching thickness of stainless steel between these coils, as the main absorber. The combined thickness of liquid hydrogen (radius of 0.4 C.L.) plus bubble chamber vacuum walls (0.3 C.L.) plus coils (3.2 C.L.) is 3.9 collision lengths, equivalent to 50 cm of iron.

Charged particles emerging from the absorber are detected by a single plane of multiwire proportional chambers that provide x, y, and diagonal coordinates for each emerging track. The proportional chambers are located just outside the bubble-chamber vacuum tank, and they are housed within the bubble-chamber building now under construction. The angular acceptances are broad and symmetric about the beam line so that both positive and negative muons from neutrino interactions are detected with good efficiency. The proportional chambers are continuously sensitive and have negligible deadtime in this application. Finally, neutrino interactions are logged in the muon identifier sequentially to reduce the confusion resulting from events uncorrelated in time.

Section II of this proposal is a brief review of the physics justification for building a muon identifier. In Section III we describe the Phase I EMI, as well as more complete versions. In Section IV we summarize test data indicating that at 4 GeV/c the Phase I EMI is already sufficient to reject pions with (94±1)% efficiency while accepting 96% of the incident muons. This can be improved to (98.5±1)% by adding 3 collision lengths externally, while a second detector plane is expected to raise the efficiency further to about 99.5%. Section V outlines the design, test, and construction program leading to the Phase I EMI and summarizes the participation of individuals and groups in the proposal.

## II. PHYSICS JUSTIFICATION

The starting point of the analysis of most bubble-chamber events that are produced by $\nu_\mu$ or $\bar{\nu}_\mu$ beams is the identification of which tracks, if any, are muons. In the method proposed here, individual tracks are measured on the bubble chamber film and are extrapolated outward until they intercept the EMI detectors. The multiple-scattering envelope containing 96% of all muons at 4 GeV/c has a radius of about 3 cm in the detector plane for the Phase I geometry. Thus incident particles that are associated with a single track within the multiple-scattering envelope are designated as muons, and all other cases are considered to be hadrons.

Among various processes that explicitly require muon identification are:

a. deeply-inelastic scattering,

b. certain intermediate-vector-boson decay modes,

c. heavy-lepton search,

d. four-Fermion interactions,

e. unusual events.

For neutrino interactions with low multiplicity, it is frequently possible to deduce the muon by its negative charge, provided the neutral beam is primarily $\nu_\mu$.[6]

In deeply-elastic scattering, the unique characteristics of the high-energy neutrino as a probe of the structure elementary particles are exploited. Two parameters are crucial in these studies: the momentum transfer $Q^2$ and the energy transfer $\nu = E-E_\mu$ from the incident neutrino to the final muon. Neither of these parameters can be determined without muon identification. Further, it is in the region where one is probing most deeply, namely the region of large momentum and energy transfers and resulting large hadron multiplicities that the identification becomes most difficult without an EMI.

Although the bubble chamber is well suited to studying the hadronic decay modes of the conjectured intermediate vector boson, analysis of the leptonic modes will depend heavily on muon identification. Calculations[7] indicate that the $\mu^-$ associated with $W^+$ production has a reasonable chance of

having a momentum of less than 1 GeV/c. It can then be trapped within the chamber and can be identified by its failure to interact. However, the $\mu^+$ from the $W^+ \rightarrow \mu^+\nu$ decay mode will be emitted at a much higher energy into the forward direction, and an auxilary means of identifying this muon is required. Scanning for these events is particularly simple: the signature is a trapped $\mu^-$.

The identification of a muon in the EMI also allows one to form the invariant mass of the muon with other detected particles, such as pions. The existence of a heavy lepton that decays into one of these combinations would be signaled by the large transverse momenta of the decay products and by a peak in the invariant mass distribution.

The four-fermion interaction, like $W^+$ production, can yield both a $\mu^-$ and a $\mu^+$. In the four-fermion case, however, both muons are likely to be highly energetic and to require auxilary identification. The EMI will greatly reduce the probability that background processes will be mistaken for this rare type of interaction.

Finally, the EMI will be invaluable in unraveling unusual and unexpected topologies. Hydrogen and, to a lesser degree, deuterium are the best target materials for uncovering such rare processes. The EMI is particularly advantageous in these cases since the external detectors preserve the entire useful volume of the bubble chamber, thereby maximizing the rate for

a given process, beam intensity, and target filling.

## III. PHASE I EXTERNAL MUON IDENTIFIER

A preliminary sketch of the "complete EMI" is shown in Fig. 1a and 1b. The complete EMI consists of: 1) a passive internal absorber filling the space between the magnet coils and matching the coil thickness in collision lengths (3.2 collision lengths stainless steel subtending up to 180° horizontally and weighing 20 tons); 2) an active detector-absorber-detector sandwich (3 collision lengths stainless steel subtending 60° vertically and up to 180° horizontally and weighing 111 tons).

The Phase I EMI, which is the subject of this proposal, consists of the passive internal absorber and a single detector plane approximating the angular acceptance of the complete EMI. This detector plane uses multiwire proportional chambers to provide x, y, and diagonal position information. By reading out high-voltage as well as ground planes, we obtain all three coordinates from a single modular layer.

The vertical distribution of muons at a radius of 3.2 meters measured from the center of the bubble chamber is shown in Fig. 2 for a 10-GeV neutrino incident. This distribution is obtained from Monte Carlo calculations and is similar for both Parton and Pomeronchuk exchange models. Less than 10% of the muons are outside ±2 meters. The complete EMI shown in Fig. 1 is centered at a radius of 3.5 meters and has a total height of 5 meters, assuring a vertical geometric

efficiency of 10% at 10 GeV.

The horizontal muon distribution is strongly influenced by the magnetic field. This is apparent in Fig. 3 where the spread in horizontal coordinates at R = 3.2 meters is given for various incident neutrino energies. An acceptance of ±90° will work well at 10 GeV and will be of some use down to 2 GeV. The geometric efficiency versus energy is plotted in Fig. 4 for an EMI with horizontal acceptance of ±90° and a vertical acceptance of ±30°, essentially the geometry shown in Fig. 1a, b.

The geometric efficiency provides an indication primarily of what fraction of the muons are subject to particle identification. By extrapolating the individual tracks observed in the bubble chamber, it will be possible to determine on a track-by-track basis precisely which tracks can be tested. In this sense, the geometric efficiency limits the muon-identification sample, but it does not restrict the identification efficiency within that sample. As already mentioned, test data relating to the identification efficiency are discussed in detail in Section IV of this proposal.

There are several major advantages that result from the use of proportional chambers as the EMI detectors: 1) proportional chambers are continuously sensitive and thus have negligible deadtime for any foreseeable neutrino flux, beam-spill duration, or bubble-chamber filling. 2) Proportional

chambers do not have to be triggered. 3) Proportional chambers can work well in high magnetic fields so that no magnetic shielding is required.

The interaction rate expected for a hydrogen filling is about 1 event per pulse, with a beam spill expected to be of order 100 μsec or less. It is not feasible to trigger large spark chambers more than once per pulse under these conditions so that even if there were no background triggers, ordinary spark chambers would have significant deadtime in the EMI application. Further, the mass of the bubble-chamber coils, coil supports, vacuum tanks, etc., is about 200 tons as compared with 1 ton for a liquid-hydrogen filling. Thus any trigger would have to reduce the background from neutrino interactions in the coils, etc., by $\sim 10^{-3}$ to be effective. Assuming this is even feasible, it clearly cannot be done without installing detectors (e.g., scintillation counters) inside the bubble-chamber vacuum tank. In this sense, the first two advantages are almost prerequisites for any EMI detector.

The third advantage, insensitivity to magnetic fields, is important when proportional chambers are compared with scintillator hodoscopes in the EMI application. To permit effective shielding of the phototubes, they would have to be located some 25 feet from the center of the bubble chamber, by which point the magnetic field will have dropped to 1 kG.

The problem is compounded by the fact that a large number ($>10^3$) of counters appear to be required to obtain the necessary spatial resolution (±2 cm).

The number of 1 $m^2$ modules needed for a single detector plane in the geometry of Fig. 1a, b is 50. The fine wires of the proportional chambers provide one coordinate, while the thicker wires of the two high-voltage planes are used to readout two coordinates at 45° to the fine-wire coordinates. If individual readouts are used, the wires will be bundled in groups small enough to yield a spatial resolution of ±2 cm. This will require about 100 readouts per 1 $m^2$ module or a total of 5000. Each group could then drive a simple amplifier + discriminator + memory element (fast shift register of 256 bits) of integrated circuit design. After each event, all shift registers are advanced 1 unit so that up to 256 events can be recorded per pulse. The shift registers are read into a Nova 800 computer and the data partially analyzed between accelerator pulses.

Electromagnetic delay lines[8] provide a promising alternative to individual-wire or wire-group readouts. The resolution required in this application (±2 cm) is well within the capability of existing delay-line systems detecting single minimizing ionizing particles. By using a buffer-storage system, it should also be possible to resolve several pulses traveling within a single delay line. Tests of various types of readout

are continuing in an effort to optimize the final design.

## IV. FEASIBILITY STUDIES

In this section, test data relating to the feasibility of an external muon identifier are summarized. The data are useful in estimating the pion rejection efficiency for both the Phase I EMI and more extensive versions. The data are derived from two sources: 1) the shower-range detector of the SLAC 20-GeV spectrometer and 2) direct measurements made at LRL using iron absorbers of different thickness with proportional chambers as detectors simulating various EMI configurations. These data imply that the proposed Phase I EMI with no external absorber will reject incident pions with (94±1)% efficiency while accepting 96% of the incident muons. A single detector plane with 3 collision lengths additional external absorber would reject pions with (98.5±1)% efficiency, while the use of two detector planes could improve this to about 99.5%.

### A. Shower-Range Data From the SLAC 20-GeV Spectrometer.

The shower-range detector in the SLAC 20-GeV spectrometer[9] is shown schematically in Fig. 5a. The detector consists of: 1) a lead-lucite shower counter with area 30 cm x 30 cm perpendicular to the beam and with a thickness of approximately 10 cm of lead and 2) a range telescope consisting of 7 iron blocks each 25 cm thick and having a width of 51 cm and a height of 76 cm. Between the shower counter and the first block of iron

there is a range counter R1, followed by 7.5 cm of lead and by a second range counter R2. The range counters beyond the first iron block are 38 cm wide and 56 cm high. Particles reaching the shower-range detector are traveling nearly parallel and are contained within an envelope 15 cm x 15 cm in cross section and within a momentum acceptance of $\Delta p/p = \pm 2\%$.

A typical printout from the shower-range detector is shown in Fig. 5b. The first column on the left, labeled SH, indicates the pulse height in the shower counter, and the row labeled R indicates the first counter in the range telescope that did not fire with a given particle incident. Thus R = 1 implies absorption in the shower counter, R = 2 implies absorption in the 7.5 cm lead block, R = 3 implies absorption in the first iron block, and so on.

Hadrons that do not interact in the shower counter have small values of the parameter SH and appear in the shower-range printout of Fig. 5b in the general area labeled NIH for non-interacting hadrons. In attempting to infer from these data something about the performance of an external muon identifier for the NAL bubble chamber, we have concentrated mainly on those hadrons that did not interact in the shower detector. Similarly, only runs with negative spectrometer settings were used, thus insuring that the great majority of the hadrons detected were pions and none were protons. Essentially then, the non-interacting sample is treated as if it were a beam of

pions incident on the 7.5 cm lead block immediately in front of the range detector.

The range data for 4.7, 7.7, 10.7, and 15.8 GeV/c pions that did not interact in the shower counter are plotted versus channel number in Fig. 6. A second horizontal scale converts channel number into the equivalent thickness of iron in cm.

The salient features of the data shown in Fig. 6 are: 1) at large thicknesses the pions are attenuated exponentially with attenuation coefficient $\lambda \approx 21$ cm (1.65 collision lengths); 2) the attenuation coefficient is virtually independent of energy, as expected from the slowly varying pion-nucleon cross section in this energy range; 3) the exponential attenuation does not set in immediately but rather is displaced due to penetrating secondaries by about 27 cm at 4.7 GeV/c, increasing to about 70 cm at 15.8 GeV/c. As discussed in Section I, this displacement is characteristic of range detectors lacking spatial resolution, and it is effectively suppressed in detectors having sufficient resolution to distinguish the large-angle scatters and the multi-prong topologies associated with hadronic interactions. In such high-resolution devices, the pion rejection varies with energy mainly through the parameter $\lambda$, which, as Fig. 6 indicates, is virtually constant.

The value of 21 cm obtained for $\lambda$ corresponds to an absorptive cross section for iron of

$$\sigma_{\pi A} \approx 38\ A^{2/3}\ \text{mb} \quad \text{(SLAC Data)}. \qquad (1)$$

Bellettini, et al.,[10] obtain for the "inelastic incoherent" proton-nucleus cross section at 20 GeV

$$\sigma_{pA}(20\ \text{GeV}) = 47.5\ A^{2/3}\ \text{mb}\ \text{(Bellettini, et al.)} \quad (2)$$

The ratio of the $\pi p$ inelastic cross section at 10 GeV to the pp inelastic cross section at 20 GeV is 21.7 mb/29.9 mb, from which we obtain an independent estimate of the pion-nucleus cross section of

$$\sigma_{\pi A}(10\ \text{GeV}) \approx \frac{\sigma_{\pi p}(10\ \text{GeV})}{\sigma_{pp}(20\ \text{GeV})}\ \sigma_{pA}(20\ \text{GeV}) \quad (3a)$$

$$\approx \frac{21.7\ \text{mb}}{29.9\ \text{mb}} \times 47.5\ A^{2/3}\ \text{mb} \quad (3b)$$

$$\sigma_{\pi A}(10\ \text{GeV}) \approx 34.5\ A^{2/3}\ \text{mb}\ \ (\text{independent estimate}). \quad (3c)$$

The agreement between the absorptive pion-nucleus cross section derived from the SLAC data and the inelastic incoherent cross section estimated from the data of Bellettini, et al., is evidently quite good.

B. Tests for an EMI Using Proportional Chambers.

A typical experimental arrangement used by us at LRL to determine the pion-rejection efficiency of muon identifiers with multiwire proportional chambers is shown schematically in Fig. 7a. In this arrangement momentum-analyzed particles from the Bevatron are incident from the left and pass through

iron absorbers, A, of various thickness before reaching the x-y proportional-chamber pairs, PC1 and PC2, with area 20 cm x 20 cm. The beam is defined initially by two counters, S1 and S2, each 12 mm x 12 mm separated by 2 m and located upstream of the apparatus shown in the figure. Two additional counters, S3 and S4, are used in conventional range studies in which the thickness of iron absorber is varied. S3 is 30 cm x 30 cm, and S4 has a width of 45 cm and a height of 55 cm.

The four proportional chambers are operated with individual wire readout[11] giving x and y coordinates at each of the two locations PC1 and PC2 indicated in the figure. The readout electronics then distinguish three types of events: 1) no charged particle detected, 2) one charged particle detected, and 3) more than one charged particle detected. Types 1 and 3 are classified separately as identified hadrons, while type 2 events are recorded on film for further analysis.

An example of the single-event x-y display transcribed from the film record is shown in Fig. 7b. In this particular run there were 1151 incident $\pi^-$ for which PC1 indicated 209 single-particle events and PC2 indicated 43 single-particle events. In addition, there were 21 multi-prong events in each detector indicating that for this geometry multiplicity is much less important than scattering angle in distinguishing hadrons. In large proportional chambers some of the events recorded as singles in this test would be classified as hadrons by multiplicity.

Single events in the PC1 and PC2 displays can also be identified as hadrons if they occur outside of the region in which incident muons would lie. This region depends to some extent on how well the incident beam direction and position are defined, but in these tests (and we assume in the actual EMI), the main limitation is multiple Coulomb scattering. The rms radius for multiple scattering at 4 GeV/c for the geometry shown in Fig. 7a is plotted versus distance in Fig. 7c. This envelope is well within the acceptances of PC1 and PC2 for all of the tests reported here; however, the acceptances of S3 and S4 are marginal at the extreme thicknesses of the range curves to be discussed shortly.

An important distinction may be helpful at this point: whereas in the conventional range detector counters of fixed area are normally used, in the high-resolution muon identifier with a single detector plane the acceptance region containing a certain percentage of muons increases with distance and with thickness due to multiple scattering. In the former case the number of surviving pions decreases exponentially because the probability of scattering out of succeeding counters of fixed area is constant. In the single-plane, high-resolution detector, the slope on a semilogarithmic plot tends to level out since the acceptance region is increasing with distance and with thickness. This means in the NAL application that the effectiveness of the external absorber is diminished if

only one detector plane is used. By sandwiching the external absorber between two high-resolution detector planes, however, one can approach the exponential case. It is fortunate in this regard that the drift space between the first absorber and the first detector plane (see Fig. 1a, b) is long since it permits an approximate redetermination at the first detector of both the particle position and the particle direction.

Figure 8 shows the range curve obtained with counters S3 and S4 and a positive beam at 4.0 GeV/c. The geometry resembles that shown in Fig. 7a except that there is no drift space between the first absorber and PC1. Nevertheless, the geometry is much less compact than that of the shower-range detector, due mainly to the presence of PC1 and PC2, and the solid angles defined by S3 and S4 are smaller in some cases by factors as large as 10. We believe that this tighter resolution, plus the somewhat lower momentum, accounts for the immediate onset of the exponential decay region.

We should note immediately that the absorptive (or inelastic incoherent) cross section alone is not sufficient to explain the immediate onset of the exponential decay region seen in Fig. 8. The dominant process for attenuating low energy secondaries in a high-resolution geometry is, in fact, nuclear multiple scattering,[12] which has an enhanced cross section in the resonance energy region. Further, since the transverse momentum per scattering is roughly constant,

the nuclear multiple scattering angles at low energy tend to be quite large.

The Bevatron beams were obtained from an external target with extracted protons of 5.9 GeV/c incident. This is only slightly above threshold for producing 4 GeV/c pions, and thus the positive beam used in these tests consists mainly of protons. The negative beam at 4.0 GeV/c is lower in intensity by a factor of order

$$\frac{\text{number } \pi^-}{\text{number p}} \approx \frac{1}{200}. \tag{4a}$$

We estimate, therefore, that the positive beam contains roughly

$$\frac{\text{number } \pi^+}{\text{number p}} \approx 2\,\frac{\text{number } \pi^-}{\text{number p}} \approx \frac{1}{100}. \tag{4b}$$

From the length of the drift space following the last bending magnet we estimate a muon component of order

$$\frac{\text{number } \mu^\pm}{\text{number } \pi^\pm} \approx \frac{1}{100}\,, \tag{4c}$$

$$\begin{aligned} \frac{\text{number } \mu^+}{\text{number p}} &\approx \left(\frac{\text{number } \mu^+}{\text{number } \pi^+}\right)\left(\frac{\text{number } \pi^+}{\text{number p}}\right) \\ &\approx \frac{1}{100} \times \frac{1}{100} \\ &\approx 10^{-4}. \end{aligned} \tag{4d}$$

This is the right order of magnitude to account for the shoulder seen in the positive range curve after 200 cm of absorber. Meanwhile, the 1% initial pion component is attenuated by more than 3 decades at 200 cm iron and is not detected.

As already mentioned, the counters S3 and S4 are not large enough to contain 100% of the muons at the extreme thicknesses of the range curve. This implies that data taken in the proportional chambers with S3 and S4 triggering on muons are somewhat biased against large-angle events. We note, however, that data taken in this way show single tracks within the muon-acceptance region of the proportional chambers with about 95% probability (i.e., with about 5% of the muon triggers yielding zero-prong or multi-prong event types). This indicates, among other things, that the track efficiency of the proportional chambers is high for the tests reported here.

Figure 9 shows the fraction of the incident particles surviving versus absorber thickness for a 4.0 GeV/c negative beam, which we believe consists mainly of pions with a 1% muon component. (The pion trigger contains a muon anti.) A surviving pion is defined in these tests as an incident beam particle that passes through the absorber and produces a single track within the multiple-scattering envelope containing a given fraction of the incident muons.

The initial attenuation length in Fig. 9 for 96% muon containment is about 15 cm corresponding to a pion nucleon

cross section of

$$\sigma_{\pi A} \approx 53\ A^{2/3}\ \text{mb} \qquad \text{(LRL Test Data)} \qquad (5)$$

This figure is remarkably high and suggests that a single-plane, high-resolution detector can be surprisingly effective at modest absorber thicknesses. The effective attenuation length for the interval 30 to 90 cm is 26 cm. The longer attenuation length in this interval is due primarily to the increasing muon multiple scattering envelope required to contain 96% of the muons.

The pion rejection efficiency indicated by Fig. 9 for the Phase I EMI is (94±1)% with 96% muon acceptance. The addition of 3 C.L. external absorber improves this rejection to (98.5±1)%. If the muon envelope is redefined by a second detector plane immediately upstream of the external absorber, we estimate that a pion rejection of 99.5% could be achieved.

## V. SCHEDULES AND FUNDING

We envision three stages in the development of the Phase I EMI. The first stage, discussed in detail in the previous section, is nearly complete and consists of testing a small version of the EMI using 0.2 m x 0.2 m multiwire proportional chambers and various thicknesses of iron in a Bevatron beam.

We view this first stage as a feasibility test in which we are primarily interested in the basic physics of muon identification: attenuation lengths, angular distributions,

hadron multiplicity, and multiple scattering. In addition, these tests have sharpened our understanding of: 1) the importance of nuclear multiple scattering in a high-resolution detector; 2) the fact that the net scattering angle, rather than particle multiplicity dominates in rejecting hadrons; 3) the distinction between a simple range detector and a high-resolution muon identifier (e.g., in the former the attenuation curve is displaced by secondaries to larger absorber thickness, while in the latter the onset of the exponential decrease occurs near zero thickness); and 4) the function of a redundant detector plane upstream (it does not reject hadrons per se, rather it reduces the muon acceptance envelope in the next detector).

The primary goal of the second stage of the Phase I EMI program is to develop an effective, inexpensive prototype module and readout system. We presently envision the prototype module as having an area 1 m x 1 m with a wire spacing of 5 mm. Our calculations indicate that at this spacing and with the normal high voltages, fine wires up to 1 m in length are stable against displacements caused by the electrostatic fields. The heavy high-voltage wires will be oriented at angles of ±45° with respect to the fine wires so that each module provides x, y, and diagonal position information. We anticipate that a total of four prototype modules will be constructed.

Several electronic readout systems are presently under consideration. In one such system, each of the prototype

modules is read out through three delay lines. The delay-line signals are then processed by pre-amps, discriminators, and position scalars, and the data are stored in a Nova 800 computer. The prompt wire signals the delayed signals from both ends of each delay line are used to resolve multiple-track ambiguities in cases in which two or more tracks from different events occur during the same delay-line readout interval. (Typical pulse speeds in such delay lines are of order 10 cm/μsec so that two particles hitting the same module within 10 μs of each other can appear on the same trace. This case can be distinguished from two particles from the same event by comparing arrival times at either end of the delay line.)

It is anticipated that the early development and construction of the prototype modules and readout electronics will occur at Berkeley and that preliminary tests will be carried out at the Bevatron. Later, when we have a working system of four modules and associated electronics, we plan to move this equipment to NAL for further testing in the neutrino beam. The detectors will be located in a Farm Equipment Shed in the neutrino beam line upstream of the bubble chamber, and the Nova 800 computer will be housed in Neutrino Lab A. (See Fig. 10)

The NAL prototype tests will use a geometry analogous to that shown in Fig. 7a. The incident tracks will be defined by two proportional-chamber modules, which simulate the bubble chamber and play the role of S1 and S2 in Fig. 7a. The two

remaining modules then simulate the two detector planes of the complete EMI and play the role of PC1 and PC2 in Fig. 7a. Additional scintillation counters will be used to check muon identification via range. In addition to testing the prototype modules, this work will provide early information about bubble-chamber backgrounds and about operating conditions in the experimental area.

The third stage is, of course, the construction and testing of the actual Phase I EMI, to be done primarily at NAL. For this purpose we request funding by NAL in the amount of $30K during the FY72 and $90K in the first half of FY73. The overall funding is summarized in Table I below. Existing cost estimates imply that we will not be able to achieve 50 $m^2$ of detector with the funds available by January 1973; however, we do expect to have an appreciable fraction of this area in operation by that date.

Table I

| Institution | Funding Agency | FY-71 | FY-72 | 1/2 FY-73 | Total Available |
|---|---|---|---|---|---|
| University of Hawaii | AEC | 38K | 120K | 80K | 238K |
| | UH | 5K | 20K | 10K | 35K |
| UCLRL | AEC | 80K | 75K | 25K | 180K |
| | UCLRL | 5K | 5K | 5K | 15K |
| NAL | AEC | 0K | 30K | 90K | 120K |

We request as part of this proposal that early hydrogen bubble-chamber film containing 1,000 neutrino interactions be

assigned to us so that we can begin as soon as possible to determine the "pull" quantities in the spatial reconstruction of the tracks. We also request an additional 10,000 neutrino interactions with the EMI to test tracking of charged particles beyond the bubble chamber wall into the EMI detectors.

We end this section by summarizing the experimental milestones:

1. Complete Bevatron EMI tests . . . . . August, 1971,
2. Complete prototype-module tests with possible continuation of NAL tests in the neutrino beam . . . . . January, 1972,
3. Complete 25% of proportional-chamber readout . . . . . July, 1972,
4. Complete Phase I EMI . . . . . January, 1973,
5. Complete bubble chamber + EMI picture taking for geometrical reconstruction . . . July, 1973.

REFERENCES

1. D. D. Jovanovic, R. Palmer, and B. Roe, "Muon Detectors After the 25-Foot Chamber," NAL 1969 Summer Study Report SS-69, Vol. II, p. 207; L. Clavelli and R. Engelman, "Theoretical Questions and Measurements of Neutrino Reactions in Bubble Chambers," NAL 1970 Summer Study Report SS-199, p. 255; R. Palmer, "Muon Detection with a Plate Inside the 15-Foot NAL Bubble Chamber," NAL 1970 Summer Study Report SS-201, p. 279; A. Mukhin and D. Yount, "External Versus Internal Muon Identification in the 15-Foot Bubble chamber," NAL 1970 Summer Study Report SS-186, p. 295.

2. NAL Proposals #9, #28, #44, #53, and #92 are among those that explicitly discuss muon identification. Others, such as NAL Proposal #45, discuss muons without mentioning identification.

3. C. Baltay, R. B. Palmer, and N. P. Samios, "Search for the Intermediate Boson, Lepton Pair Production, and a Study of Deeply Inelastic Reactions Utilizing High Energy Neutrino Interactions in Liquid Neon," NAL Proposal #53.

4. M. L. Stevenson et al., "Proposal for a High-Energy Neutrino Experiment in the NAL 30 $m^3$ $H_2$, $D_2$ Bubble Chamber," NAL Proposal #9.

5. A report of the NAL Fifteen-Foot Bubble Chamber Workshop has been widely circulated by J. R. Sanford of NAL, beginning April 23, 1971.

6. M. L. Stevenson, 200 GeV Experimental Use, Vol. 2, UCID-10152, 86 (1966). This possibility is also discussed in the various NAL Summer Studies and Proposals already referenced.
7. R. W. Brown, R. H. Hobbs, and J. Smith (to be published). See also D. Cline, A. K. Mann, and C. Rubbia, Phys. Rev. Letters 25, 1309 (1971) and M. L. Stevenson, "High Energy Neutrino Physics (E > 20 GeV) and the Constraints Placed on the Detectors," 1969 NAL Summer Study, Vol. 2, 121 (1969).
8. R. Grove, I. Ko, and V. Perez-Mendez, Nucl. Instr. and Methods 89, 257 (1970), "Phase Compensated Delay Lines for Wire Chamber Readout."
9. A. Boyarski, SLAC-PUB-559 (1969). Also S. Eklund (private communication). We are grateful for the use of these unpublished data.
10. Bellettini et al., Nucl. Phys. 79, 609 (1966).
11. The readout electronics was kindly loaned to us by H. Steiner.
12. A. Citron, L. Hoffmann, C. Passow, W. R. Nelson, and M. Whitehead, Nucl. Instr. and Methods 32, 48 (1965).

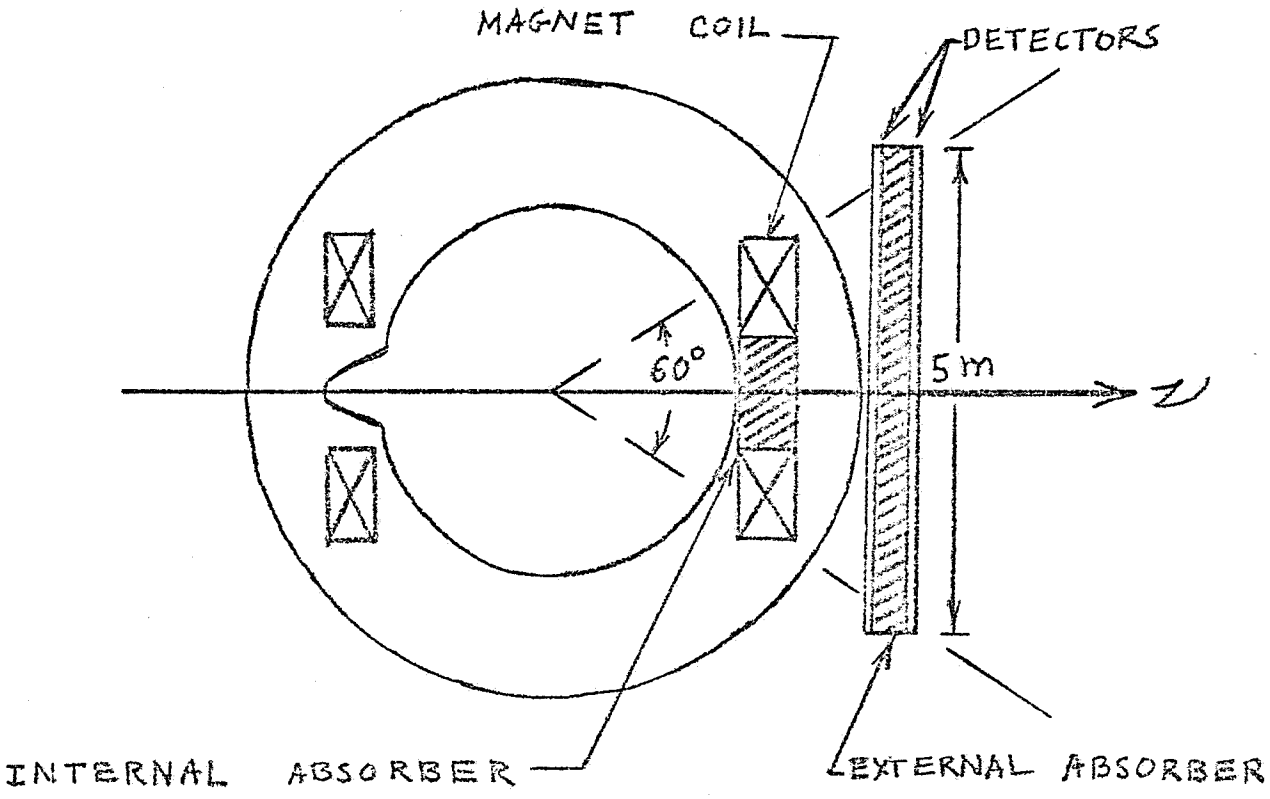


Fig. 1 a BUBBLE CHAMBER AND EMI, SIDE VIEW

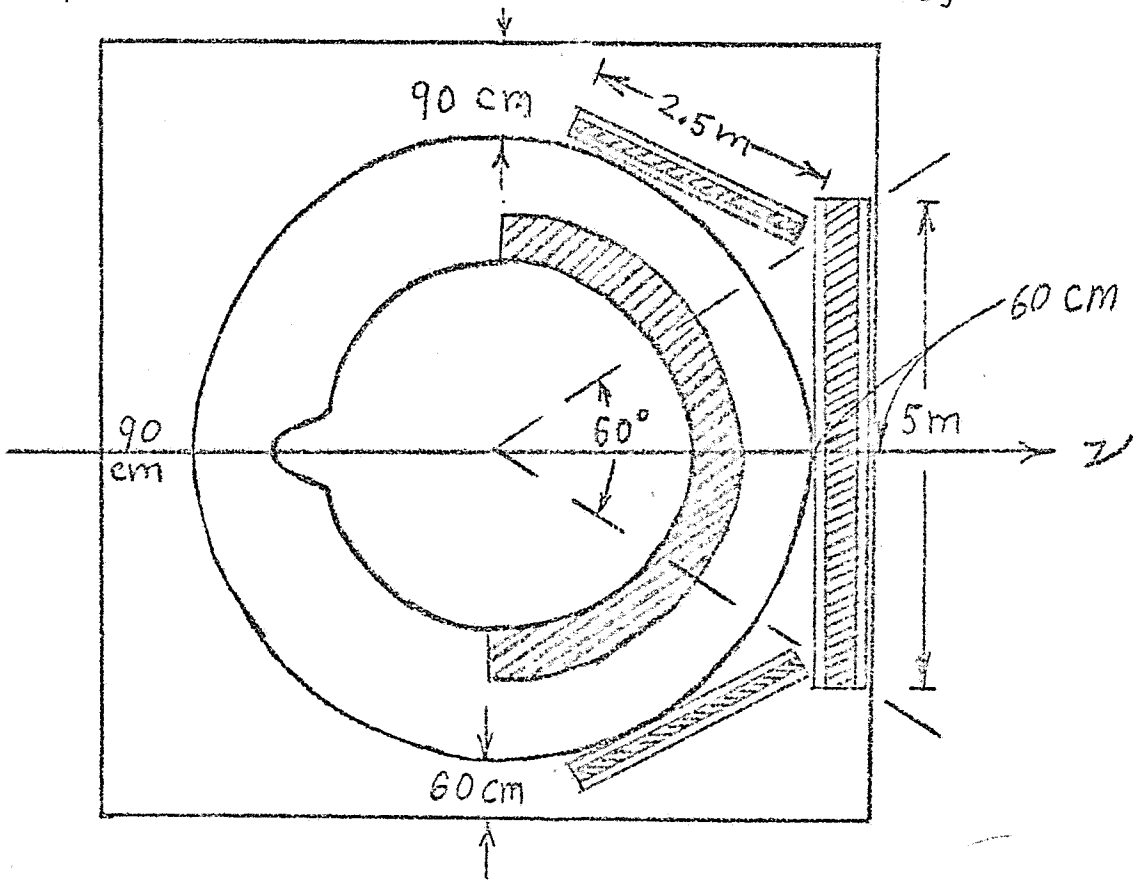


Fig. 1 b BUBBLE CHAMBER AND EMI, TOP VIEW

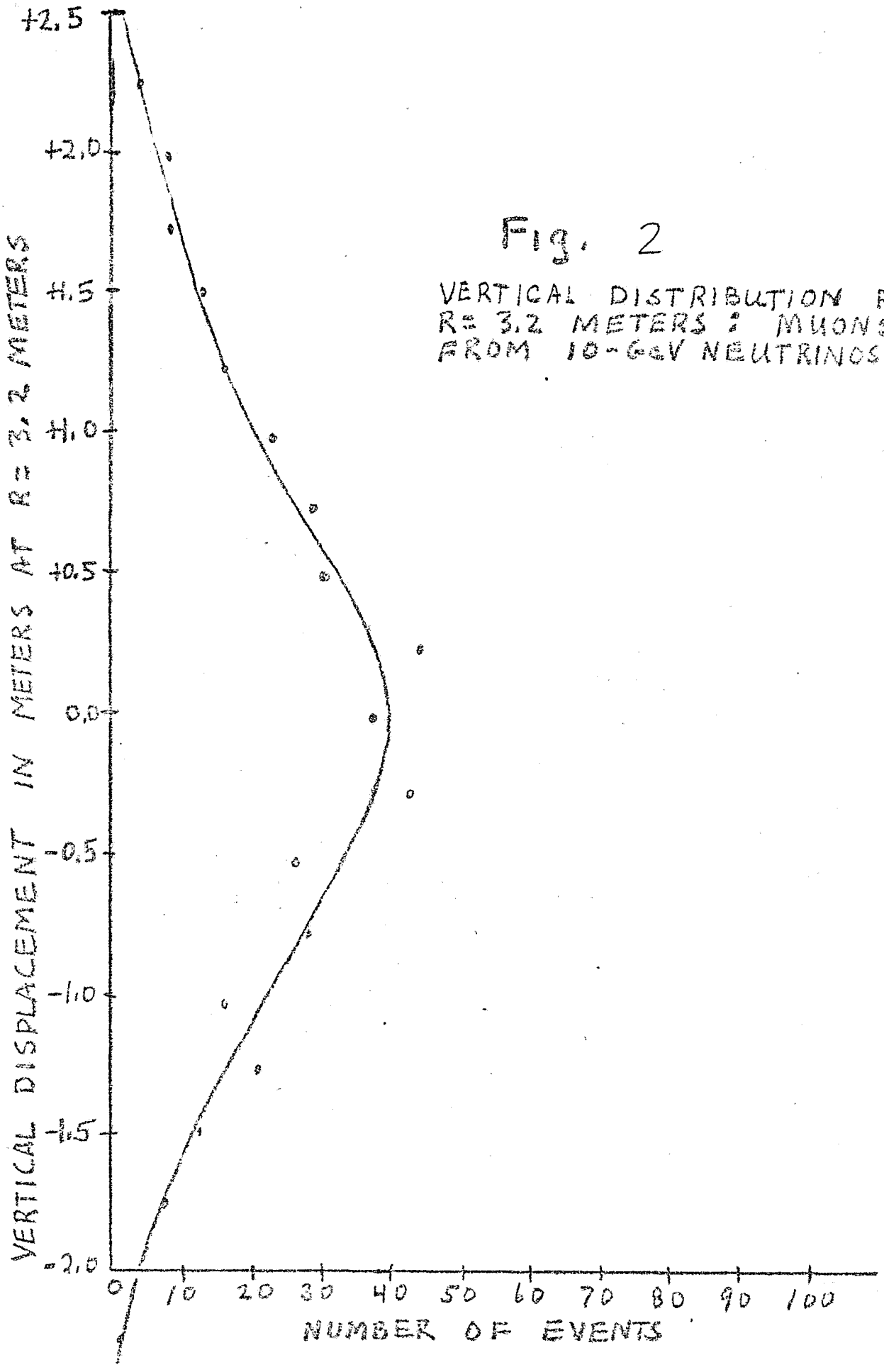


Fig. 2

VERTICAL DISTRIBUTION AT R = 3.2 METERS : MUONS FROM 10-GeV NEUTRINOS

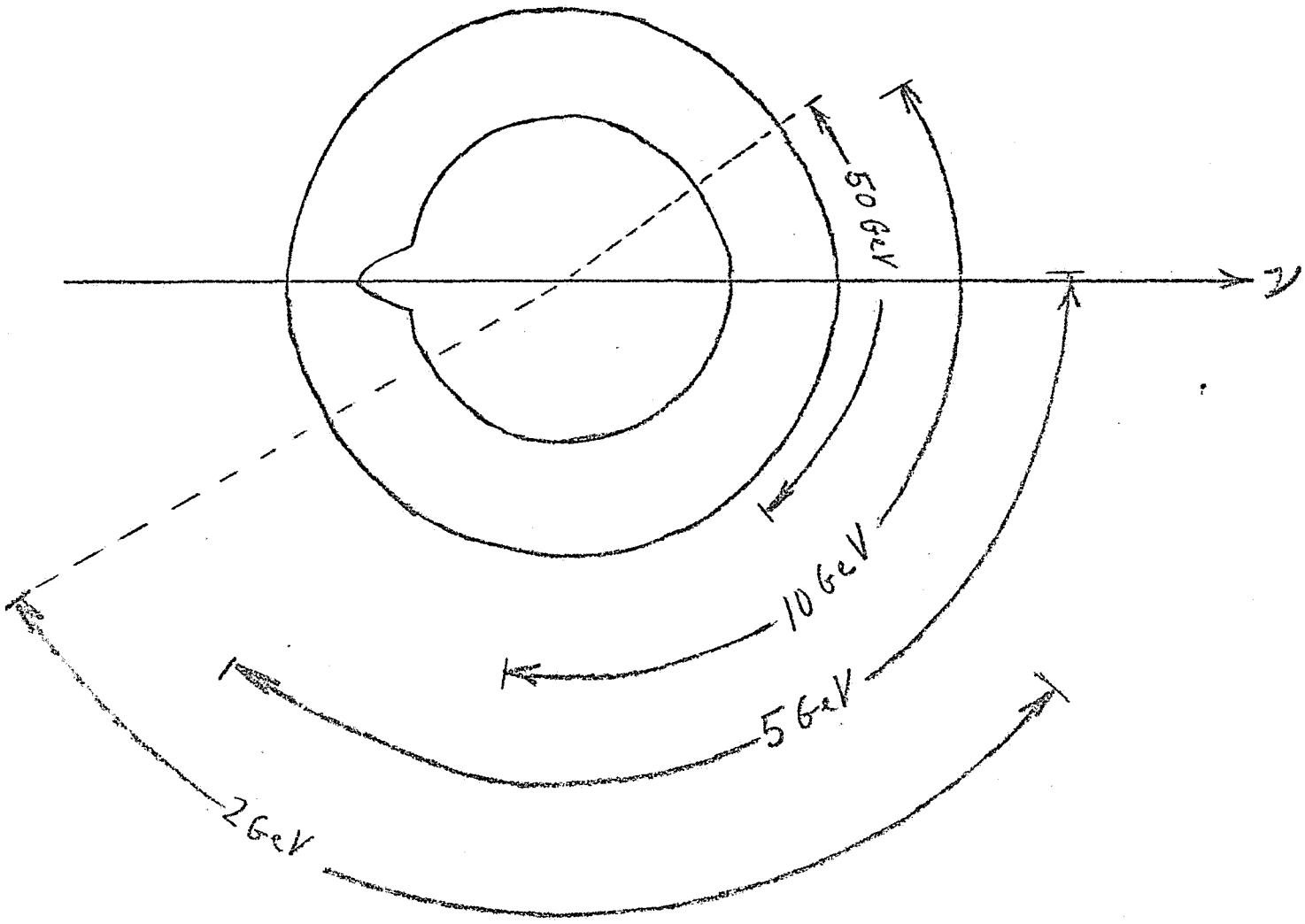


Fig. 3 HORIZONTAL DISTRIBUTION OF MUONS AT R = 3.2 METERS

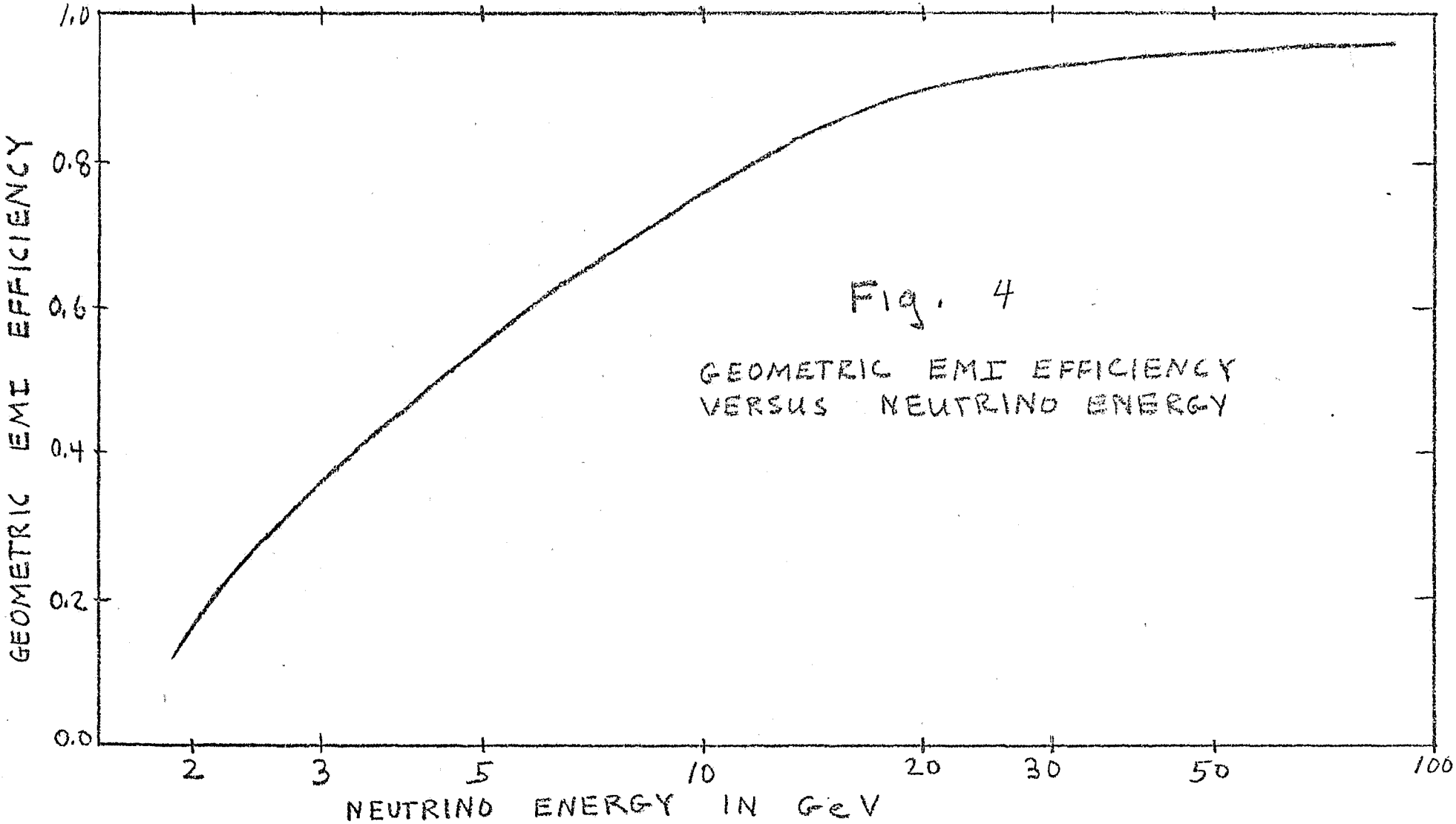


Fig. 4

GEOMETRIC EMI EFFICIENCY
VERSUS NEUTRINO ENERGY

Fig. 5

5a.

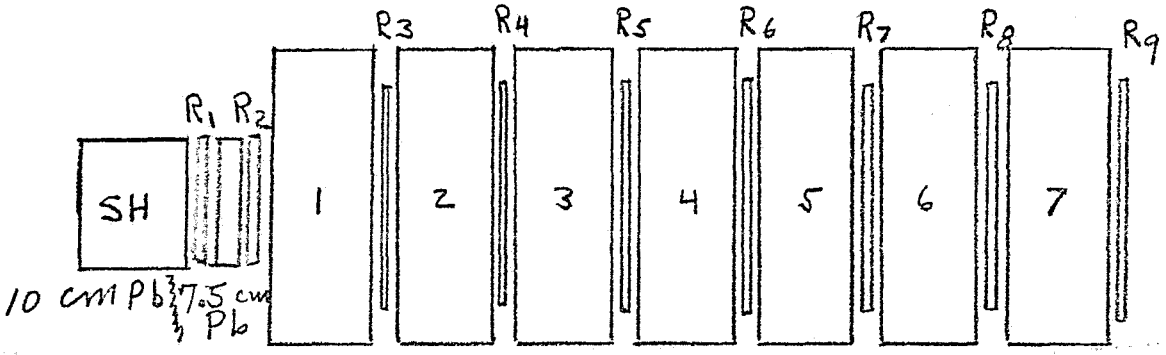


7 BLOCKS IRON EACH 10" THICK

5b.

| SH | R = 1 | 2 | 3 | 4 | 5 | 6 | 7 | 8 | 9 | 10 |
|---|---|---|---|---|---|---|---|---|---|---|
| 0 | 0 | 0 | 0 | 0 | 0 | 0 | 0 | 0 | 0 | 0 |
| 2 | 0 | 0 | 0 | 0 | 0 | 0 | 0 | 0 | 0 | 0 |
| 4 | 0 | 0 | 0 | 0 | 0 | 0 | 0 | 0 | 0 | 0 |
| 6 | 0 | 0 | 0 | 0 | 0 | 0 | 0 | 0 | 0 | 0 |
| 8 | 0 | 0 | 0 | 0 | 0 | 0 | 0 | 0 | 0 | 0 |
| 10 | 4456 | 53 | 39 | 23 | 7 | 5 | 1 | 3 | 0 | 1 |
| 12 | 644 | 22 | 11 | 9 | 0 | 0 | 0 | 0 | 0 | 0 |
| 14 | 217 | 10 | 10 | 4 | 2 | 0 | 0 | 0 | 0 | 0 |
| 16 | 169 | 6 | 7 | 2 | 3 | 0 | 0 | 0 | 0 | 1 |
| 18 | 157 | 67 | 631 | 1196 | 563 | 182 | 64 | 22 | 31 | 290 |
| 20 | 219 | 382 | 2610 | 4410 | 2076 | 666 | 187 | 73 | 124 | 1052 |
| 22 | 236 | 272 | 1360 | 1955 | 903 | 268 | 102 | 33 | 54 | 469 |
| 24 | 150 | 141 | 553 | 658 | 268 | 77 | 20 | 11 | 23 | 145 |
| 26 | 149 | 70 | 257 | 263 | 112 | 35 | 8 | 3 | 5 | 55 |
| 28 | 134 | 74 | 179 | 139 | 71 | 14 | 5 | 0 | 4 | 31 |
| 30 | 137 | 60 | 154 | 140 | 40 | 13 | 2 | 0 | 2 | 10 |
| 32 | 133 | 50 | 122 | 118 | 37 | 7 | 4 | 1 | 1 | 9 |
| 34 | 137 | 42 | 103 | 93 | 15 | 10 | 1 | 0 | 2 | 10 |
| 36 | 129 | 63 | 107 | 79 | 22 | 8 | 1 | 1 | 0 | 5 |
| 38 | 122 | 53 | 108 | 82 | 10 | 8 | 1 | 1 | 0 | 4 |
| 40 | 728 | 301 | 476 | 306 | 94 | 16 | 8 | 0 | 0 | 2 |
| 50 | 852 | 355 | 479 | 249 | 76 | 16 | 9 | 1 | 1 | 2 |
| 60 | 993 | 380 | 435 | 230 | 48 | 8 | 2 | 1 | 0 | 3 |
| 70 | 1243 | 402 | 387 | 192 | 35 | 6 | 2 | 0 | 0 | 0 |
| 80 | 1394 | 398 | 336 | 150 | 33 | 3 | 1 | 0 | 0 | 0 |
| 90 | 1410 | 361 | 287 | 118 | 24 | 4 | 1 | 1 | 0 | 0 |
| 100 | 1359 | 329 | 248 | 95 | 8 | 2 | 0 | 0 | 0 | 0 |
| 110 | 1191 | 258 | 202 | 50 | 8 | 0 | 0 | 0 | 0 | 0 |
| 120 | 1010 | 196 | 120 | 38 | 5 | 2 | 0 | 0 | 0 | 1 |
| 130 | 878 | 159 | 100 | 25 | 4 | 1 | 0 | 0 | 0 | 0 |
| 140 | 1198 | 158 | 55 | 11 | 2 | 0 | 0 | 0 | 0 | 0 |
| 150 | 1310 | 121 | 23 | 9 | 1 | 0 | 0 | 0 | 0 | 0 |
| 160 | 10 | 1 | 1 | 0 | 1 | 0 | 0 | 0 | 0 | 0 |
| 170 | 2 | 1 | 0 | 1 | 0 | 0 | 0 | 0 | 0 | 1 |
| 180 | 3 | 0 | 0 | 0 | 1 | 0 | 0 | 0 | 0 | 0 |
| 190 | 5 | 0 | 0 | 0 | 0 | 0 | 0 | 0 | 0 | 0 |
| 200 | 3 | 0 | 0 | 0 | 0 | 0 | 0 | 0 | 0 | 0 |
| 210 | 2 | 0 | 0 | 0 | 0 | 0 | 0 | 0 | 0 | 0 |
| 220 | 0 | 0 | 0 | 0 | 0 | 0 | 0 | 0 | 0 | 0 |
| 230 | 1 | 0 | 1 | 0 | 0 | 0 | 0 | 0 | 0 | 0 |
| 240 | 0 | 0 | 0 | 0 | 0 | 0 | 0 | 0 | 0 | 0 |
| 250 | 0 | 0 | 0 | 0 | 0 | 0 | 0 | 0 | 0 | 0 |

NIH

Fig. 6

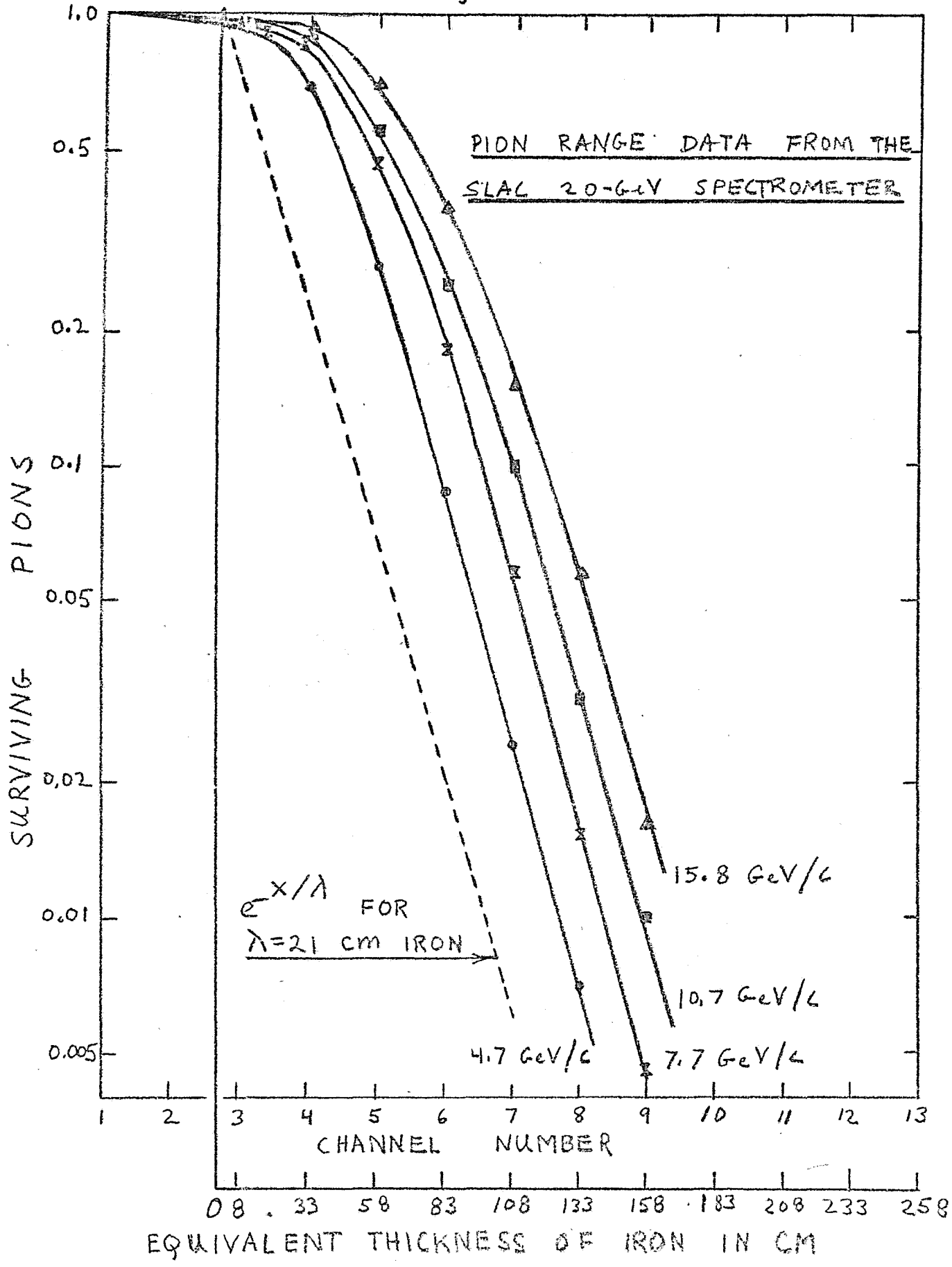
PION RANGE DATA FROM THE SLAC 20-GeV SPECTROMETER
SURVIVING PIONS
1.0
0.5
0.2
0.1
0.05
0.02
0.01
0.005
$e^{-x/\lambda}$ FOR $\lambda$=21 cm IRON
15.8 GeV/c
10.7 GeV/c
7.7 GeV/c
4.7 GeV/c
1 2 3 4 5 6 7 8 9 10 11 12 13
CHANNEL NUMBER
0 8 . 33 58 83 108 133 158 183 208 233 258
EQUIVALENT THICKNESS OF IRON IN CM

Fig. 7

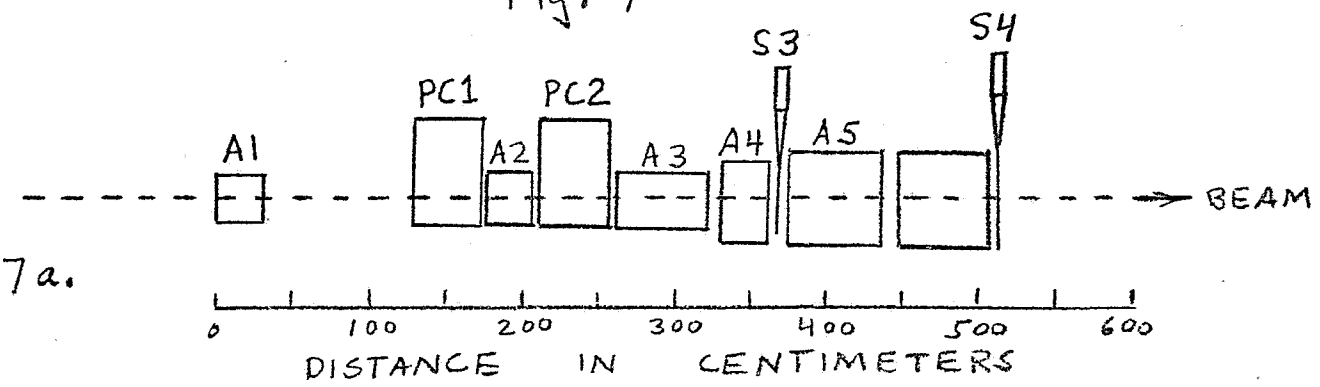
S3
S4
PC1
PC2
A1
A2
A3
A4
A5
BEAM

7a.


0
100
200
300
400
500
600
DISTANCE IN CENTIMETERS

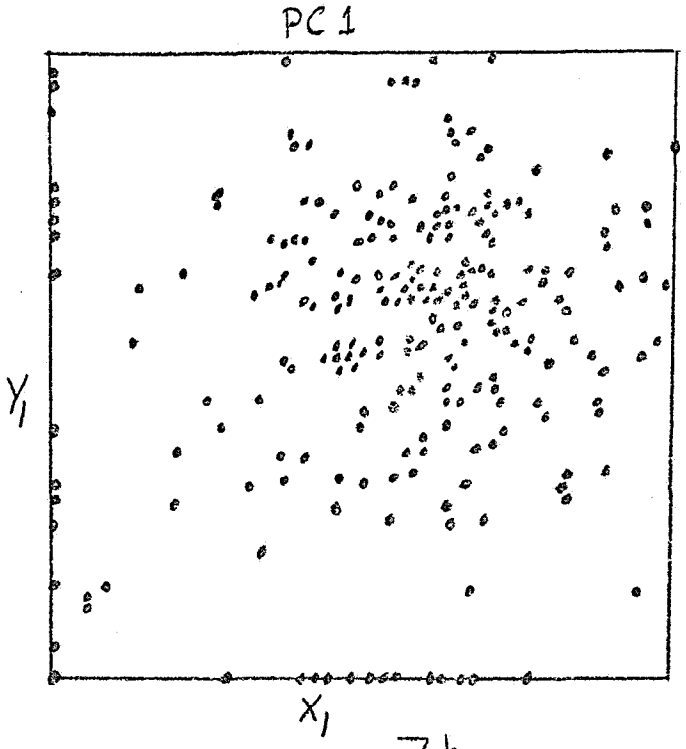
PC 1
$Y_1$
$X_1$

7b.

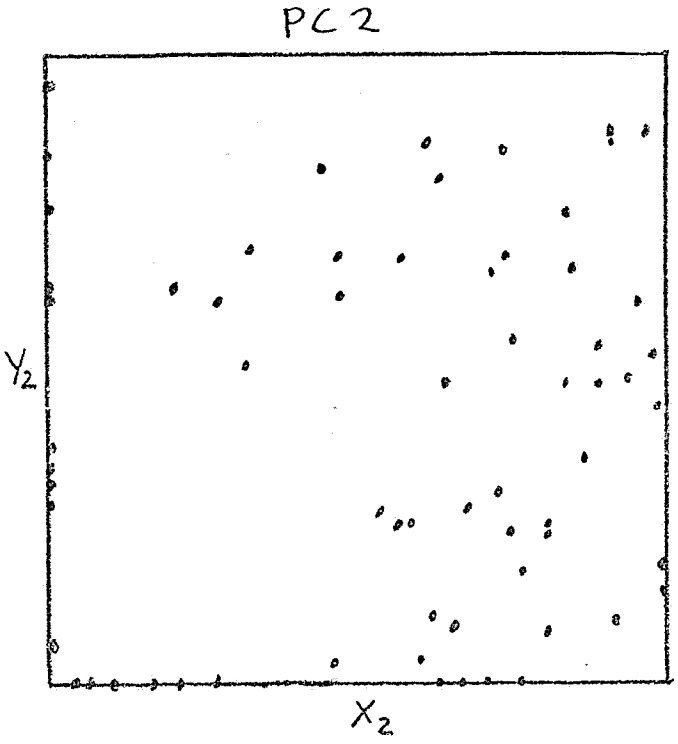
PC 2
$Y_2$
$X_2$

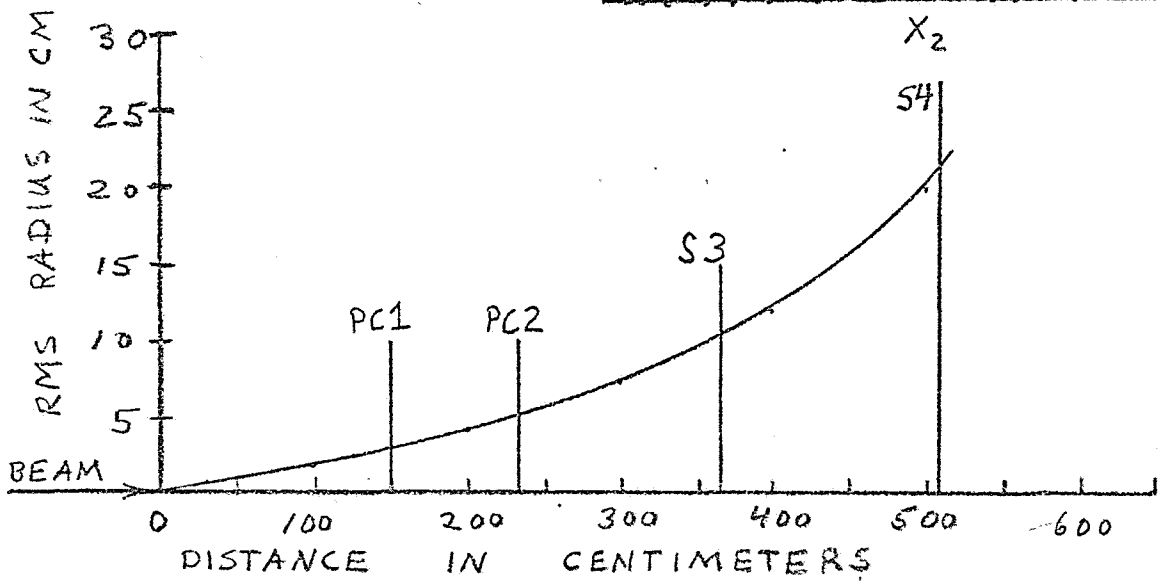
RMS RADIUS IN CM
30
25
20
15
10
5
BEAM
S4
S3
PC1
PC2
0
100
200
300
400
500
600
DISTANCE IN CENTIMETERS

7c.

Fig. 8

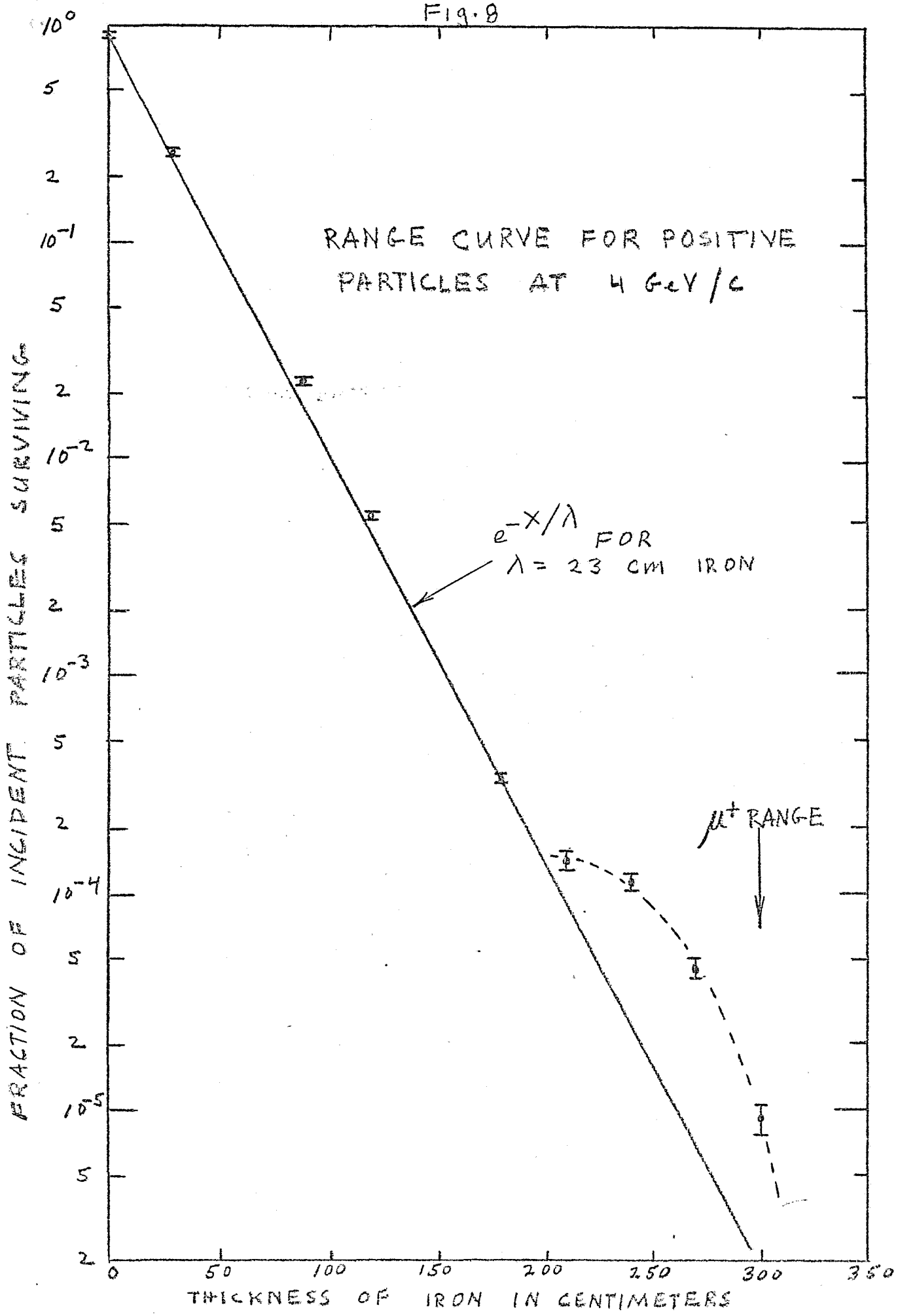
RANGE CURVE FOR POSITIVE PARTICLES AT 4 GeV/c
$e^{-x/\lambda}$ FOR $\lambda$ = 23 cm IRON
$\mu^+$ RANGE
FRACTION OF INCIDENT PARTICLES SURVIVING
THICKNESS OF IRON IN CENTIMETERS
$10^0$
5
2
$10^{-1}$
5
2
$10^{-2}$
5
2
$10^{-3}$
5
2
$10^{-4}$
5
2
$10^{-5}$
5
2
0
50
100
150
200
250
300
350

Fig. 9

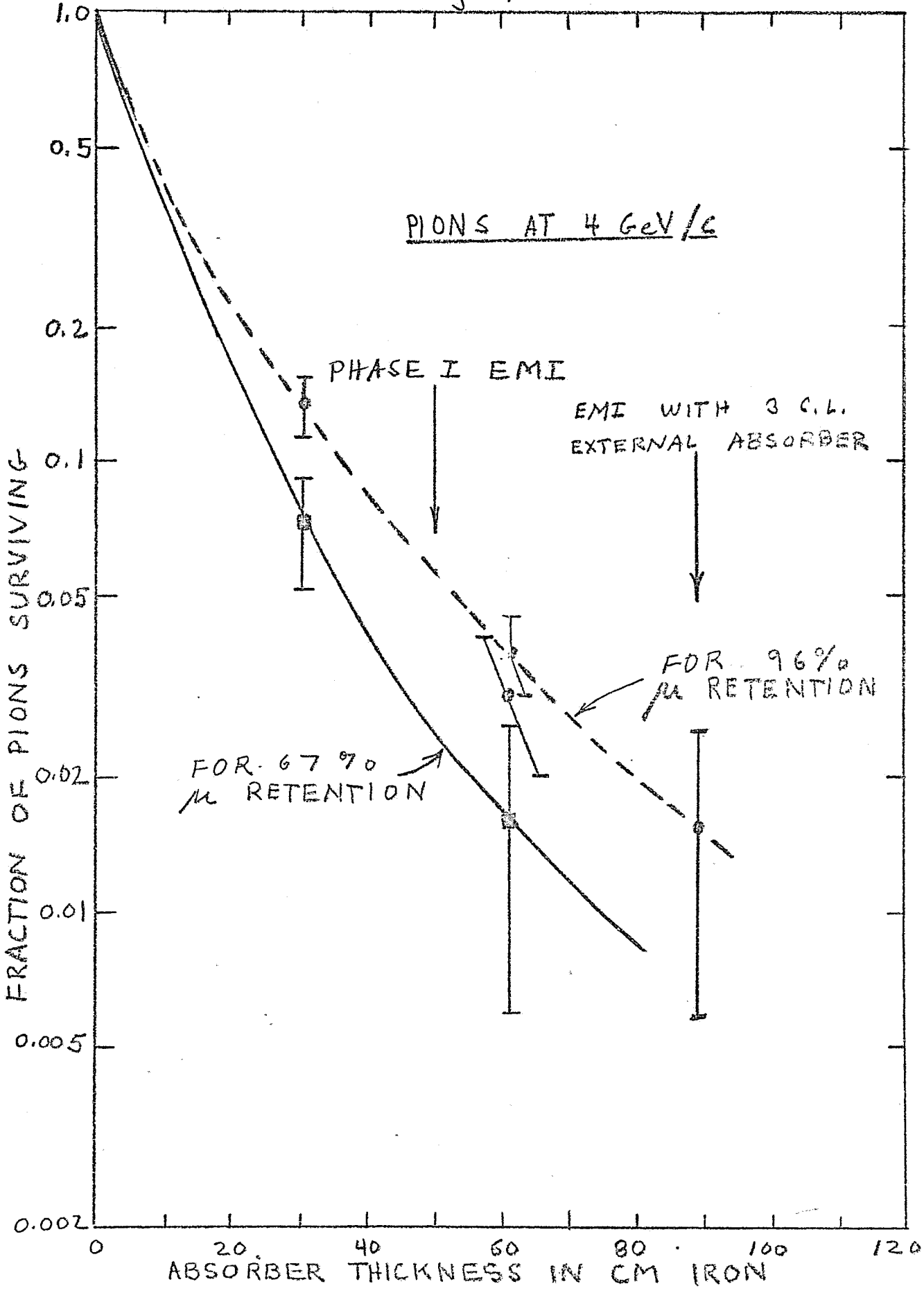
PIONS AT 4 GeV/c
PHASE I EMI
EMI WITH 3 C.L. EXTERNAL ABSORBER
FOR 96% μ RETENTION
FOR 67% μ RETENTION
FRACTION OF PIONS SURVIVING
1.0
0.5
0.2
0.1
0.05
0.02
0.01
0.005
0.002
0
20
40
60
80
100
120
ABSORBER THICKNESS IN CM IRON

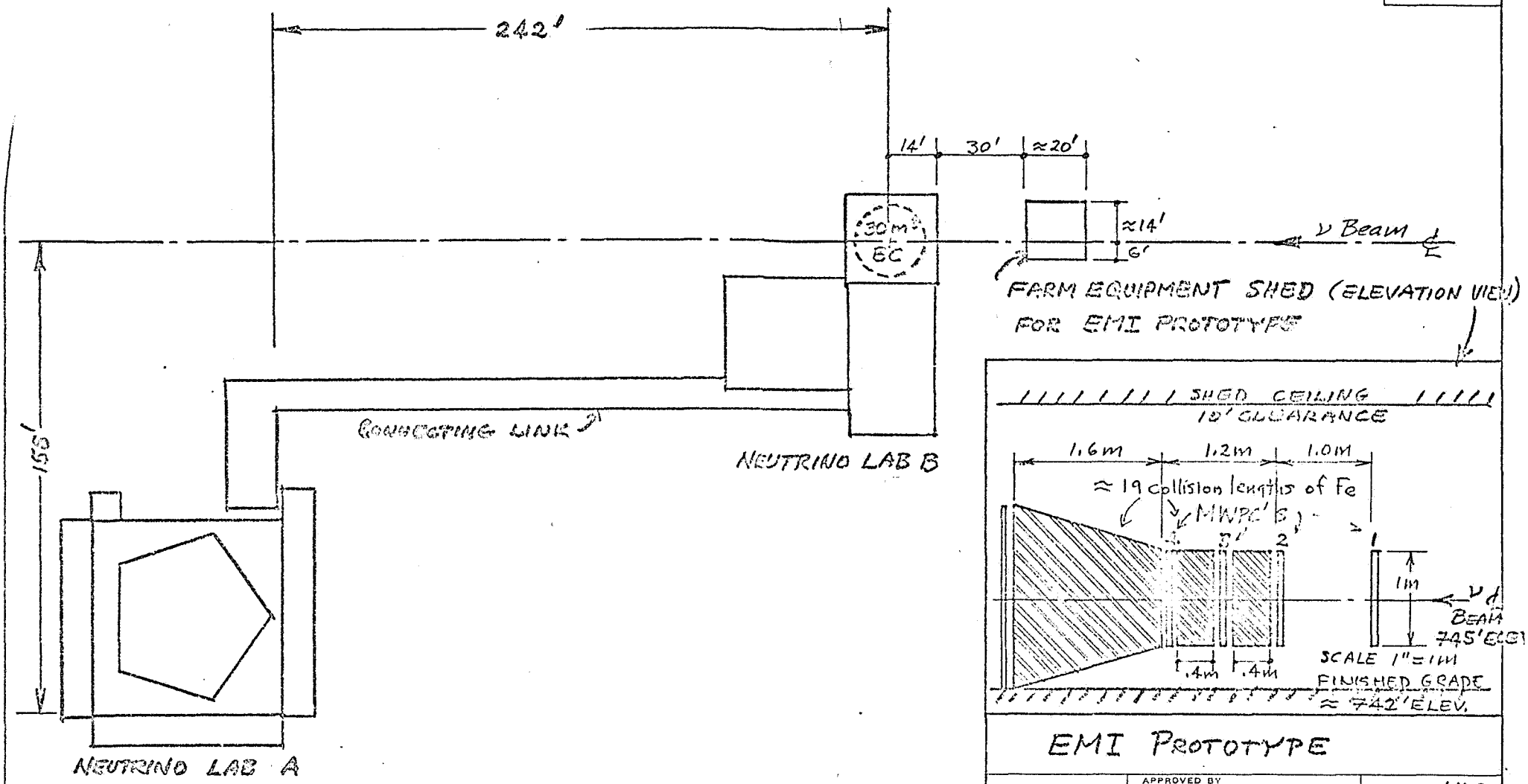


# EMI PROTOTYPE

| SCALE: | APPROVED BY | DRAWN BY MLS |
|---|---|---|
| DATE: 21 Jun 71 | | |

NAL PROPOSAL No. 9c

DRAWING NUMBER Fig. 1'